arXiv:1603.02647v1 [cond-mat.quant-gas] 8 Mar 2016

Finite Temperature Phase Transitions in the SU(N) Hubbard model

Hiromasa Yanatori and Akihisa Koga
Department of Physics, Tokyo Institute of Technology, Tokyo 152-8551, Japan
(Dated: March 9, 2016)

We investigate the SU(N) Hubbard model for the multi-component fermionic optical lattice system, combining dynamical mean-field theory with the continuous-time quantum Monte Carlo method. We obtain the finite temperature phase diagrams with $N \leq 6$ and find that low temperature properties depends on the parity of the components. The magnetically ordered state competes with the correlated metallic state in the system with the even number of components ($N \geq 4$), yielding the first-order phase transition. It is also clarified that, in the odd-component system, the ordered state is realized at relatively lower temperatures and the critical temperature is constant in the strong coupling limit.

Ultracold atomic systems have potential to understand some important and fundamental issues in the condensed matter physics [1–3]. Among them, two-component fermionic systems with distinct hyperfine states are known to be appropriate to describe strongly correlated electron systems. Owing to the high controllability in particle number, lattice potential, and interaction strength, remarkable phenomena have been observed such as superfluid state [4, 5], BCS-BEC crossover [6, 7] and Mott insulating state [8, 9]. Recently, the multicomponent fermionic systems are realized such as the three components ^{6}Li [10], six components ^{173}Yb [11] and ten components ^{87}Sr [12]. This stimulates further theoretical investigations on fundamental problems [13, 14].

One of the interesting systems is the optical lattice system, which is realized by loading the ultracold atoms in a periodic potential. This ideal system should be described by the SU(N) Hubbard model, and its ground states have been discussed such as the dimerized state in the one dimension [15–18], the staggered flux order in two dimensions [15, 19], and some translational symmetry breaking states and the superconducting states in the infinite dimensions [20–25]. However, systematic studies for finite temperature properties are still lacking [25, 26]. In particular, it is unclear how the stability of the ordered states depends on the parity of the components, which should be important to observe the spontaneously translational symmetry breaking state in the fermionic optical lattice experiments [27].

Motivated by this, we consider the SU(N) Hubbard model,

$$\hat{\mathcal{H}} = -t \sum_{\langle i,j\rangle,\alpha} c^{\dagger}_{i\alpha} c_{j\alpha} + \frac{U}{2} \sum_{i} n_i^2, \tag{1}$$

where $n_i = \sum_\alpha n_{i\alpha}$ is the total number density of fermions at the ith site, $\langle i,j\rangle$ indicates the nearest neighbor sites and $c^{\dagger}_{i\alpha}(c_{i\alpha})$ creates (annihilates) a fermion with "color" $\alpha(=1,2,\cdots,N)$ at site i and $n_{i\alpha} = c^{\dagger}_{i\alpha} c_{i\alpha}$. t is the hopping integral and U is the on-site interaction between fermions with distinct components. Setting chemical potential $\mu = NU/2$, we discuss the particle-hole symmetric systems.

We examine low temperature properties in the system by means of dynamical mean-field theory (DMFT) [28–30], which maps the lattice model to the problem of a single-impurity connected dynamically to an effective medium. The Green's function is obtained via the self-consistency conditions imposed of the impurity problem. We present the fermion band by a semicircular density of state (DOS) $\rho(\epsilon) = 2\sqrt{1-(\epsilon/D)^2}/(\pi D)$, where D is the half-bandwidth.

In the paper, we consider the translational symmetry breaking state in the bipartite lattice as one of most probable candidates. Then, the self-consistent equations [31] are given by, $\mathcal{G}_{\gamma\alpha}(i\omega_n) = i\omega_n + \mu - (D/2)^2 G_{\bar{\gamma}\alpha}(i\omega_n)$, where $G_{\gamma\alpha}(\mathcal{G}_{\gamma\alpha})$ is the full (noninteracting) Green function with color α for the $\gamma(=A,B)$th sublattice. To solve the effective impurity problem, we make use of the hybridization-expansion continuous-time quantum Monte Carlo (CTQMC) method [32, 33], which should be suitable for systematic investigations on the Hubbard model.

To discuss how stable the spontaneously translational symmetry breaking states are at finite temperatures, we calculate the staggered order parameters $m_\alpha = \langle n_{A\alpha} - n_{B\alpha}\rangle/2$, where $n_{\gamma\alpha}$ is the number operator for color α in the γth sublattice. In the system, the possible ordered states depend on the parity of the components. When the number of component is even, we expect that the repulsive interaction stabilizes the "antiferromagnetically" (AF) ordered state, where the $N/2$ fermions occupies at the A sublattice and the others at the B sublattice. Schematic pictures for $N = 2$ and 4 are shown in Figs. 1(a) and (b). In the case, the order parameters can be defined as $m = m_1 = m_2 = \cdots = m_{N/2} = -m_{N/2+1} = \cdots = -m_N$. In the odd component system, some ordered states should be realizable. For examples, in the three component system, the color density wave (CDW) and color-selective antiferromagnetically ordered (CSAF) states are degenerate at zero temperature [42], as shown in Figs. 1 (c) and (d). In the former state, the order parameters have the relation $m_1 = m_2 \neq m_3$, while $m_1 = -m_2$ and $m_3 = 0$ in the other. Therefore, we care-

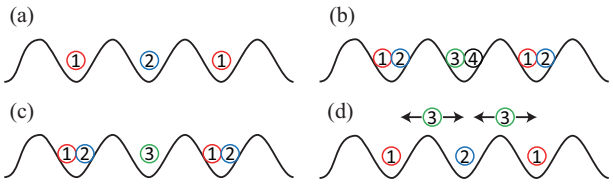

FIG. 1: (Color online) (a) AF state for $N = 2$. (b) AF state for $N = 4$. (c) CDW state for $N = 3$. (d) CSAF state for $N = 3$.

fully study the stability of possible ordered states in the multicomponent fermionic systems.

Let us consider the system with the even components ($N = 2M$), which is equivalent to the Hubbard model with M-fold degenerate bands [37, 38, 41]. We show the order parameters in the systems with $N = 2, 4$, and 6 at the temperature $T/D = 0.02$. When $N = 2$ ($M = 1$),

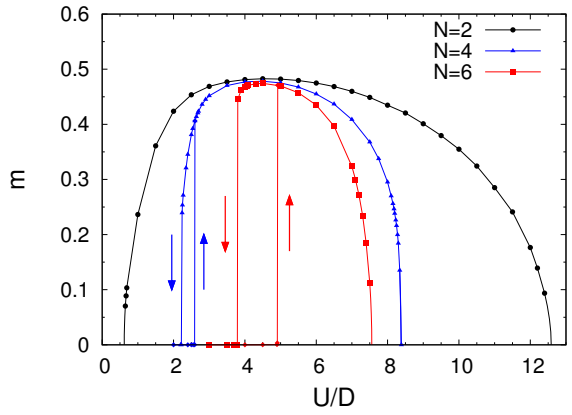

FIG. 2: (Color online) Order parameters m as functions of the repulsive interaction U/D when $T/D = 0.02$. Lines are guides to the eye. The arrows indicate the existence of a hysteresis in the order parameters.

the system is reduced to the single-band Hubbard model. The normal metallic state is realized in the weak coupling region. Increasing the repulsive interaction, the order parameter is induced at a certain critical interaction U_{c1} and the AF state is realized. Furthermore, increasing the interaction, the order parameter has a maximum around $U/D \sim 4$, and decreases. Finally, it vanishes at another critical interaction U_{c2}, where the second-order phase transition occurs. The critical values are deduced as $(U/D)_{c1} \sim 0.62$ and $(U/D)_{c2} \sim 12.6$, by examining critical behavior $m \sim |U - U_c|^\beta$ with the exponent $\beta = 1/2$ [34].

When $N \geq 4$ ($M \geq 2$), the nature of the phase transition in the strong coupling region is not changed. The critical interaction is slightly decreased since the characteristic energy decreases as $\sim N/(N-1)\cdot D^2/U$. Namely, these critical values are deduced as $(U/D)_c \sim 8.4$ for $N = 4$ and 7.6 for $N = 6$. However, in the weak coupling region, different behavior appears. Increasing the interaction, a jump singularity appears in the order parameter at $(U/D) \sim 2.6$ ($N = 4$) and 4.9 ($N = 6$), as shown in Fig. 2. On the other hand, decreasing the interaction from the AF state, the order parameter vanishes at $(U/D) \sim 2.2$ ($N = 4$) and 3.8 ($N = 6$). The hysteresis means the existence of the first-order phase transition in the even-component system with $N \geq 4$.

By performing similar calculations, we obtain the finite temperature phase diagrams for $N = 2, 4$ and 6, as shown in Fig. 3. It is found that in the two-component

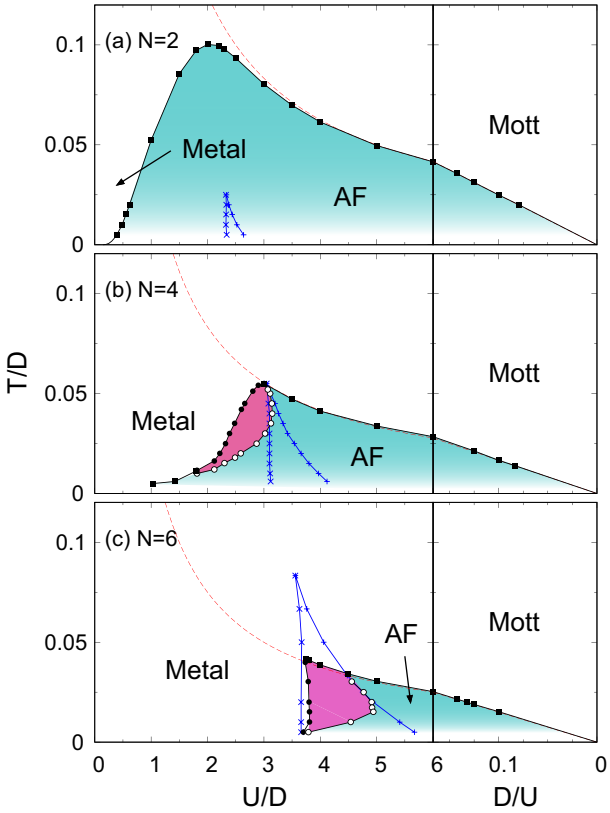

FIG. 3: (Color online) Phase diagrams for the multicomponent systems with $N = 2, 4$, and 6. Solid squares represent the second-order magnetic phase transition points. Open (solid) circles represent the transition points, where the normal (AF) state disappears. Dashed lines represent the phase boundaries $ND^2/8(N-1)U$ obtained by means of the strong coupling expansion. Pluses (crosses) represent the transition points under the paramagnetic condition, where metallic (Mott insulating) state disappears.

system, the AF state is widely stabilized at finite temperatures. We also examine low temperature properties under the paramagnetic condition. Here, we calculate $z = (1 - \mathrm{Im}\Sigma_\alpha(i\omega_0)/\omega_0)^{-1}$ as a renormalization factor at finite temperatures, where Σ_α is the selfenergy for color α and $\omega_0 = \pi T$. It is found that the Mott phase boundaries [35], where a jump singularity appears in z, are

much lower than the magnetic one. This is consistent with the fact that no Mott transitions are realized in the bipartite system with $N = 2$ [36].

As increasing N, the Mott critical temperature is increased [37, 38], in contrast to the decrease of the magnetic transition temperature. When $N = 4$, the Mott transition temperature is comparable to the maximum of the magnetic transition, as shown in Fig. 3 (b). We find that, in the weak and strong couping regions, the second-order phase transition occurs. On the other hand, the first-order phase transition occurs in the intermediate coupling region ($2 \lesssim U/D \lesssim 3$). To clarify how particle correlations affect the phase transitions, we show in Fig. 4 the temperature dependence of the order parameter and renormalization factor. It is known that the latter is appropriate to discuss particle correlations characteristic of low energy properties. In the weak coupling region, the renormalization factor is large and the normal metallic state is realized above the critical temperature $(T/D) \sim 0.011$. In the AF state ($T < T_c$), the order parameter gradually increases. In the intermediate coupling region $U/D = 2.6$, different behavior appears. Decreasing temperatures, the renormalization factor decreases toward zero, implying that insulating behavior appears when $T/D > 0.2$. However, it has a minimum around $T/D \sim 0.1$ and takes a larger value $z \sim 0.4$ near the first-order transition temperature. This means the crossover from the insulating state to the metallic state. It is known that, in the two-band system ($M = 1$), this correlated metallic state close to the Mott transitions is stabilized due to the enhancement of spin and orbital fluctuations [39, 40]. At lower temperatures, the jump singularity appears in the order parameter and the AF state is realized. In the case, the large gap suddenly appears in the DOS (not shown). Therefore, in the intermediate coupling region, the first-order magnetic transition occurs together with the metal-insulator transition. In the strong coupling region with $U/D = 5.0$, critical behavior clearly appears around $(T/D)_c \sim 0.034$. When $T > T_c$, the renormalization factor is small enough to realize the Mott insulating state.

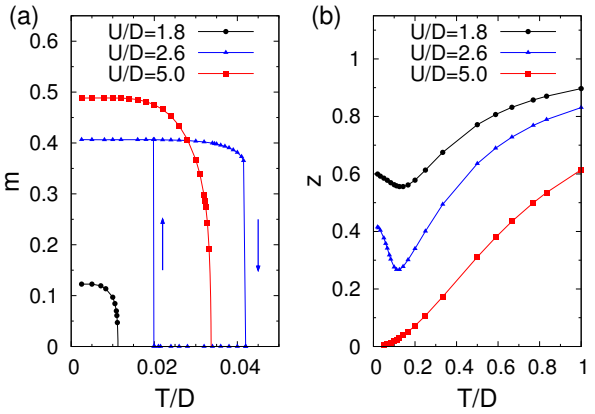

FIG. 4: (Color online) Order parameter m (a) and renormalization factor z (b) as functions of temperature for the four component systems when $U/D = 1.8, 2.6$, and 5.0.

In the system with $N = 6$, the Mott critical temperature is higher than the magnetic transition temperature, as shown in Fig. 3(c). Therefore, the Mott transition indeed occurs when the interaction strength is changed at the intermediate temperature $0.04 \lesssim T/D \lesssim 0.08$. We also find that the metallic state is stable up to a fairly large interacting region at finite temperatures. Then, the phase transition from the metallic (Mott) state to the AF state is of first (second) order. These results are essentially the same as those for the $N = 4$ system.

In the even-component system with a large N, the correlated metallic state becomes more stable against the magnetic instability. Roughly speaking, the metallic state is realized in the weak coupling region until the Mott transition, which are characterized by three values: the boundaries for the coexisting region between metallic and Mott insulating states at zero temperature U_{c1} and U_{c2} ($U_{c1} < U_{c2}$), and the critical end point (U_c, T_c). It is known that U_{c2} is proportional to the number of components N [37, 38, 41], while the others are the square root of N [37, 38]. On the other hand, the AF state is realized at low temperatures $T \lesssim ND^2/8(N-1)U$ in the strong coupling region ($U \gtrsim U_{c2}$). We conclude that, in the large N case, the phase diagram is similar to that for the $N = 6$ system and the first-order phase transition between the correlated metallic and AF states occurs in the intermediate coupling region.

Now, we turn to the multicomponent system with $N = 2M + 1$. For convenience, we focus on the system with $N = 3$ ($M = 1$). It has been clarified that the CDW and CSAF states, which are schematically shown in Figs. 1(c) and (d), are degenerate at zero temperature [42]. We have performed the detailed CTQMC calculations to deduce the critical temperatures for both states, and little difference between them has been found. Therefore, in the following, we only show the results for the CSAF state to discuss the stability of the ordered states in the system.

Fig. 5 shows the order parameter m in the three-component system. When $T/D = 0.02$, the ordered state is realized in the intermediate region $1.5 \lesssim U/D \lesssim 10.8$. The result is similar to magnetic behavior in the two-component system, where the phase transitions are of second order. On the other hand, decreasing temperature, different behavior appears in the strong coupling region, as shown in Fig. 5. When $T/D = 0.015$, the increase in the interaction U decreases the order parameter m slowly. We find no phase transition to the paramagnetic state, at least, until $U/D \leq 256$. At the lower temperature $T/D = 0.01$, the order parameter should be finite even in the strong coupling limit, as shown in

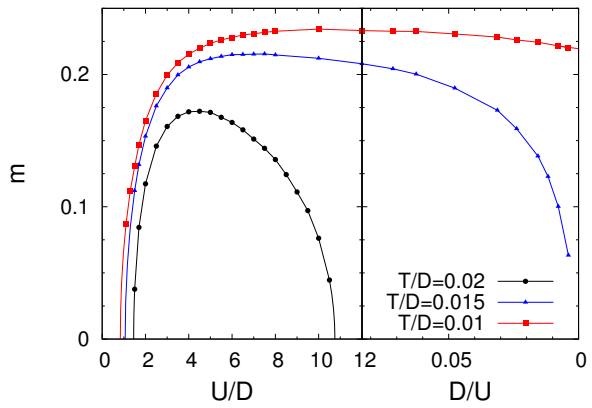

FIG. 5: (Color online) Order parameters m as functions of the repulsive interaction U/D in the three component system when $T/D = 0.01, 0.015$, and 0.02.

Fig. 5.

We obtain the phase diagrams in the systems with $N = 3$ and 5, as shown in Fig. 6. In the $N = 3$

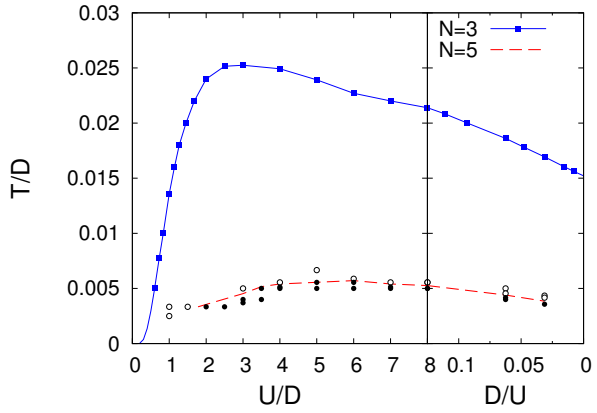

FIG. 6: (Color online) Phase diagrams for the odd-component systems with $N = 3$ and 5. Solid (open) circles indicate the state with (without) the order parameter for the $N = 5$ system. The phase boundaries are guides to the eyes.

system, the transition temperature takes the maximum $T/D \sim 0.025$ around $U/D = 2.5$, which is relatively lower than the phase boundaries for the even-component system discussed before. The increase in the interaction strength decreases the critical temperature monotonically. By extrapolating the phase boundary, we obtain a finite critical temperature $(T/D)_c \sim 0.015$ ($\sim 1/64$) in the limit $U \to \infty$. This remarkable behavior should be explained by the following. When one considers the CSAF state [Fig. 1(d)], a fermion in the doubly occupied sites can hop freely to the nearest neighbor singly occupied sites and the metallic state is realized even in the strong coupling limit [43]. This is contrast to the even-component system, where the corresponding energy cost is proportional to the onsite interaction strength U. This should suggest that the effective intersite interaction between the localized spins ($S_i^\gamma = \sum_{\alpha,\beta=1,2} c_{i\alpha}^\dagger \sigma_{\alpha\beta}^\gamma c_{i\beta}$) is proportional to the bandwidth, resulting in the finite critical temperature $T_c(\propto D)$. This may recall us the Bose-Einstein condensation in a free bosonic system since the transition temperature does not depend on the interaction strength. Therefore, it may allow us to discuss the BCS-BEC crossover in the two-component Fermi gas, which is now under consideration.

An ordered state is also realized in the system with $N = 5$. In the case, the transition temperature is much lower than that for the $N = 3$ system, as shown in Fig. 6. Therefore, we could not determine the phase boundary accurately. However, the ordered state, shown as solid circles in Fig. 6, is realized even in the strong coupling region. Therefore, we believe that such low temperature properties are common to the half-filled odd-component system.

We have investigated the phase transitions in the multi-component fermion system, combining dynamical mean-field theory with the hybridization-expansion continuous-time quantum Monte Carlo method. The finite temperature phase diagrams have been obtained for the Hubbard model with $N(\leq 6)$ components. We have found that the magnetically ordered state competes with the correlated metallic state in the system with the even number of components. We have clarified that, in the system with the odd number of components, the critical temperature is relatively lower than that for the even number cases. In addition, we have found that the critical temperature is finite even in the strong coupling limit.

Acknowledgments

The authors would like to thank J. Nasu and P. Werner for valuable discussions. This work was partly supported by the Grant-in-Aid for Scientific Research from JSPS, KAKENHI No. 25800193 (A.K.). The simulations have been performed using some of the ALPS libraries [44].

[1] I. Bloch, Nature Physics **1**, 23 - 30 (2005)
[2] U. Schneider, L. Hackermüller, S. Will, Th. Best, I. Bloch, T. A. Costi, R. W. Helmes, D. Rasch, A. Rosch, Science **322** (2008) 1520
[3] I. Bloch, J. Dalibard and S. Nascimbène Nature Physics **8**, 267 (2012).
[4] S. Jochim, M. Bartenstein, A. Altmeyer, G. Hendl, S. Riedl, C. Chin, J. Hecker Denschlag, and R. Grimm, Science **302** 2101 (2003).
[5] M. W. Zwierlein, C. A. Stan, C. H. Schunck, S. M. F. Raupach, S. Gupta, Z. Hadzibabic, and W. Ketterle, Phys. Rev. Lett. **91**, 250401 (2003).

[6] T. Bourdel, L. Khaykovich, J. Cubizolles, J. Zhang, F. Chevy, M. Teichmann, L. Tarruell, S. J. J. M. F. Kokkelmans, and C. Salomon, Phys. Rev. Lett. **93**, 050401 (2004).

[7] C. A. Regal, M. Greiner, and D. S. Jin, Phys. Rev. Lett. **92**, 040403 (2004).

[8] R. Jördens, N. Strohmaier, K. Günter, H. Moritz, and T. Esslinger, Nature **455**, 204 (2008).

[9] U. Schneider, L. Hackermüller, S. Will, Th. Best, I. Bloch, T. A. Costi, R. W. Helmes, D. Rasch, and A. Rosch, Science **322**, 1520 (2008).

[10] T. B. Ottenstein, T. Lompe, M. Kohnen, A. N. Wenz, and S. Jochim, Phys. Rev. Lett. **101**, 203202 (2008).

[11] T. Fukuhara, Y. Takasu, M. Kumakura, and Y. Takahashi, Phys. Rev. Lett. **98**, 030401 (2007).

[12] B. J. DeSalvo, M. Yan, P. G. Mickelson, Y. N. Martinez de Escobar, and T. C. Killian, Phys. Rev. Lett. **105**, 030402 (2010).

[13] T. Paananen, J.-P. Martikainen, and P. Törmä, Phys. Rev. A **73**, 053606 (2006).

[14] P. F. Bedaque and J. P. D'Incao, Ann. Phys. **324**, 1763 (2009).

[15] J. B. Marston and I. Affleck, Phys. Rev. B **39**, 11538 (1989).

[16] N. Kawakami, Phys. Rev. B **47**, 2928 (1993).

[17] R. Assaraf, P. Azaria, M. Caffarel, and P. Lecheminant, Phys. Rev. B **60**, 2299 (1999).

[18] K. Buchta, Ö. Legeza, E. Szirmai, and J. Sólyom, Phys. Rev. B **75**, 155108 (2007).

[19] C. Honerkamp and W. Hofstetter, Phys. Rev. Lett. **92**, 170403 (2004).

[20] T. Momoi and K. Kubo, Phys. Rev. B **58**, R567 (1998).

[21] K. Inaba and S. I. Suga, Phys. Rev. Lett. **108**, 255301 (2012).

[22] Y. Okanami, N. Takemori, and A. Koga, Phys. Rev. A **89**, 053622 (2014).

[23] A. Koga and P. Werner, Phys. Rev. B **91**, 085108 (2015).

[24] S. Hoshino and P. Werner, Phys. Rev. Lett. **115**, 247001 (2015).

[25] H. Yanatori and A. Koga, J. Phys. Soc. Jpn. **85**, 014002 (2016).

[26] K. Inaba and S. Suga, Mod. Phys. Lett. B **27**, 1330008 (2013).

[27] R. A. Hart, P. M. Duarte, T.-L. Yang, X. Liu, T. P. E. Khatami, R. T. Scalettar, N. Trivedi, D. A. Huse and R. G. Hulet, Nature **519**, 211 (2015).

[28] W. Metzner and D. Vollhardt, Phys. Rev. Lett. **62**, 324 (1989).

[29] A. Georges, G. Kotliar, W. Krauth, and M. J. Rozenberg, Rev. Mod. Phys. **68**, 13 (1996).

[30] T. Pruschke, M. Jarrell, and J. K. Freericks, Adv. Phys. **44**, 187 (1995).

[31] R. Chitra and G. Kotliar, Phys. Rev. Lett. **83**, 2386 (1999).

[32] P. Werner, A. Comanac, L. déMedici, M. Troyer, and A. J. Millis, Phys. Rev. Lett. **97**, 076405 (2006).

[33] E. Gull, A. J. Millis, A. N. Rubtsov, A. I. Lichtenstein, M. Troyer, and P. Werner, Rev. Mod. Phys. **83**, 349 (2011).

[34] A. Koga and P. Werner, Phys. Rev. A **84**, 023638 (2011).

[35] R. Bulla, T. A. Costi, and D. Vollhardt, Phys. Rev. B **64**, 045103 (2001).

[36] R. Zitzler, N.-H. Tong, T. Pruschke, and R. Bulla, Phys. Rev. Lett. 93, 016406 (2004).

[37] N. Blümer and E. V. Gorelik, Phys. Rev. B **87**, 085115 (2013).

[38] K. Inaba, A. Koga, S. I. Suga, and N. Kawakami, Phys. Rev. B **72**, 085112 (2005).

[39] A. Koga, Y. Imai, and N. Kawakami, Phys. Rev. B **66**, 165107 (2002).

[40] A. Koga, T. Ohashi, Y. Imai, S. Suga, and N. Kawakami, J. Phys. Soc. Jpn. **72**, 1306 (2003).

[41] Y. Ono, M. Potthoff, and R. Bulla, Phys. Rev. B **67**, 035119 (2003).

[42] S. Y. Miyatake, K. Inaba, and S. I. Suga, Phys. Rev. A **81**, 021603 (2010).

[43] K. Inaba, S. Y. Miyatake, and S. I. Suga, Phys. Rev. A **82**, 051602 (2010).

[44] B. Bauer, L. D. Carr, H. G. Evertz, A. Feiguin, J. Freire, S. Fuchs, L. Gamper, J. Gukelberger, E. Gull, S. Guertler, A Hehn, R. Igarashi, S. V. Isakov, D. Koop, P. N. Ma, P. Mates, H. Matsuo, O. Parcollet, G. Pawłowski, J. D. Picon, L. Pollet, E. Santos, V. W. Scarola, U. Schollwöck, C. Silva, B. Surer, S. Todo, S. Trebst, M. Troyer, M. L. Wall, P Werner, and S. Wessel, J. Stat. Mech. P05001 (2011).